Internal waves generation and decay in Celtic Sea

Dmitry Aleynik and Mark Inall
Scottish Association for Marine Science, Scottish Marine Institute,
Oban, Argyll, PA37 1QA, UK. email: dmitry.aleynik@sams.ac.uk

Introduction. Based on a review of ancient eclipse observation (*1*) and the correspondent slow-down of Earth's rotation rate, the suggestion is that Moon tidal acceleration (measured with precise accuracy in modern times (*2*)), are attributed mostly to tidal energy dissipation in the oceans, with smaller contributions (<6%) from the mantle, solid earth crust, atmosphere and, a controversial effect, to variations (not only glacial) of the Earth's equatorial oblateness. From total tidal energy dissipation (3.7TW if solar tide included) the loss due to Internal Tide (IT) generation in deep ocean was generally under-estimated (10%), as has been recognized (*3*). Since global satellite data of sea surface elevation become available for assimilation in tidal models, the area with significant topographically related IT generation attributes ~30% of tidal energy dissipation *(4)*, (*5*). About 10% (266GW) of the global lunar flux dissipates in Celtic and North seas (*6*). Internal gravity waves are generated in stratified waters by the interaction of barotropic tidal currents with uneven sea bed topography. This process contributes to the dissipation of tidal energy and enhances mixing in deep ocean and in shelf waters. How much energy is lost locally and how much propagates coastward in the one of the world's most energetic areas is in a focus of this research.

A promising way of parameterising the dissipative effects of vertical mixing in the shelf seas, which still remain a sub-grid process for the most of ocean numerical models, is in the reliable estimates of internal wave's energy decay rate, based on measurements and considered as approximately equal to the measured dissipation rate. Remote sensing data reveal coherent propagations of IT energy across Celtic sea for hundreds kms (*7*),while the estimates of IT e-folding decay rate based on spatial coherence, derived from discrete observations, varies in other locations from 35 (*8*) to 85 km (*9*), the latter probably overestemated (*10*). Simultaneous quasi-synoptic velocity and hydrography sections were recognised recently as a reliable tool to determine the structure, and to quantify the decay rate of the internal tide across a broad continental shelve, e.g. in the Celtic Sea. With these observations the first *in situ* evidence of a coherent IT signal is detected over many (*five*) wavelengths along 170 km line from shelf edge toward the shore, and the cross-shelf energy decay scale is estimated as 42 km. The wavelength-averaged dissipation rate inferred from this decay 2.08×10^{-7} Wkg^{-1} which is close to local tidally- and vertically-averaged estimate from micro-structure measurements.

Observations and instrumentation. Two-dimensional hydrographic data from a 250 km long transect "TR1" from the shelf-break toward Jones Bank (JB) were obtained over 16.3 hours on 25/26th July 2008 [*Figure 1a*] with a Seabird 911 CTD mounted on a Scanfish platform undulating with a two minutes cycle through water column from 5m below surface to 10m above sea bottom and towed at a speed of 4.4 $m\cdot s^{-1}$ at a distance 500-800m behind the ship during the James Cook 25th Cruise. A vessel mounted 150 kHz ADCP measured the absolute horizontal velocity averaged in 2-minutes ensembles and 4-m bins at depth range from 14m from surface to 15m above the sea bed. Both hydrography and velocity data have been gridded onto an xz-plane with resolution 750×2m in an identical fashion using linear distance weighting with search radii sx=500m, sz=4m.

Analysis. The wavelength of the dominant quasi-periodic perturbation (10-15m in amplitude) of the σ_θ*=26.7 isopycnal* was of about 35 km (*Figure 1b*), while the spectrum of its displacement anomaly has the highest pick at 41 km. Using the mid-shelf density profile from CTD 041 and the internal wave vertical structure equation, the phase speed of the fundamental M2 internal tide was C_p=0.78 ms^{-1} with a wavelength of 35 km. The propagating baroclinic signal is Doppler shifted relative the known velocity of moving vessel (4.4 $m\cdot s^{-1}$) to the wave phase speed. Close values of dynamical mode estimate (35km) and Doppler-corrected wavelength (33.5km) give the evidence that the pycnocline perturbations are associated with low mode IT propagating along the transect TR1. Strong evidence in a favour of remote generation of these pycnocline perturbations versa local topographic generation are revealed in the ADCP data. The former (remote) one required fixed phase relationship between amplitude and velocity of propagating internal waves, and definitely the mode 1 waves looks nearly stationary for the ship moving 6 times faster than the mode 1 phase (1/6 Doppler red-shift). The vertical transect of decomposed across-slope baroclinic velocity $u'(z,x)= u(z,x) - \langle u\rangle_z$, revealed pronounced beam-like V-shape structure (*Figure 1c*) at distance 50-160 km (directly above shelf break (SB) and shoreward), with smaller signal at 160-245 km (SW from JB), where $u(z,x)$ is measured and $\langle u\rangle_z$ is the vertically averaged (barotropic) velocities (*Figure 1c*). The theoretical trajectory of M2 internal wave energy propagation path in a stationary stratified sea, calculated using the formula for angle α to the horizontal: $\alpha = \frac{(\omega - \langle u\rangle_z(x)\cdot k)^2 - f^2}{N^2 - (\omega - \langle u\rangle_z(x)\cdot k)^2}$, where k is the horizontal wavenumber of the mode 1 internal waves ($k=2\pi$/33.5km), ω is the M_2 tidal frequency, f and N are the Coriolis and the stratification parameters, was plotted as a bold line (*Figure 2c*). Two separate energy propagating rays paths are shown: one starts above SB (52 km), the other starts directly above JB (195 km). SB domination in IT generation is confirmed with a calculation the IT-generating vertical body force $F(x)$ (over a tidal period) using (*11*) formulation with reasonable smoothing of the seabed slope (33 km low-pass filter applied, as we are focusing on mode 1 waves). Also proportional translation over 5 wavelength periods (~3-days) for reducing of tidal volume flux $Q(t)$ was applied. The highest peak (>6 times the elsewhere values) was found over the shelf-break with smaller peak over JB. Using the approach of (*12*) we estimate the total baroclinic $E(\lambda)$, Kinetic KE and Available Potential APE energy density distribution along the transect averaging within each of the λ=1–6 segments corresponding to one IT wavelength as defined by the ray paths, also scaled for taking into account reducing in body force since the start of propagation of the 1st of 5 IT waves. The highest scaled energy density $E(\lambda)=0.0135\,m^2s^{-2}$ (13.9 Jm^{-3}) was found in an over SB segment (centred at 75 km), with 66% contribution from KE, and over slopes JB (0.0045 m^2s^{-2} or 4.6 Jm^{-3}), where APE dominates (84%). For the first 5 independent values of $E(\lambda)$ the exponential fit ($R=0.95$) gives an e-fold scale of b_λ= 42 km.

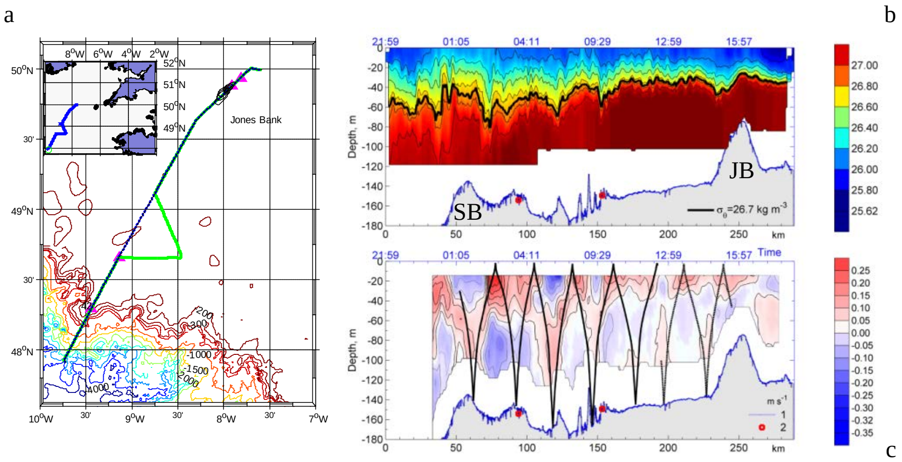

Figure 1. (a) Celtic Sea bathymetry and RRS James Cook ship track TR1 (green) and the same section geometrically adjusted (dashed blue) assuming long wavelength internal tide propagating with phase lines parallel to SB. (b) Vertical slice of potential density σ_θ along section TR1 as a function of distance from SB. Search radii sz = 4 m, sx = 0.5 km, and grid dx = 0.75 km, dz = 2 m. (c) Vertical distribution of the along-section baroclinic velocity. Superimposed are the Doppler shifted theoretical ray traces for an M2 period internal wave.

References

1. E. Hadley. *Phil Trans*, **19**, 160-175 (1695).
2. J. O. Dickey *et al. Science*, **265**, 482 (1994).
3. C. Wunsch. *Rev of Geophys*, **13**, 167 (1975).
4. G. D. Egbert, R. D. Ray. *J of Geophys Res*, **106**, 22475 (2001).
5. C. Garrett, E. Kunze. *Annual Rev of Fluid Mech*, **39**, 57 (2007).
6. W. Munk. *Progr in Oceanog*, **40**, 7 (1997).
7. R. D. Pingree, A. L. New. *Deep-Sea Res. Part I - Oc Res Papers*, **42**, 245 (1995).
8. E. L. Shroyer, J. N. Moum, J. D. Nash. *Nonlin Proc in Geophys*, **17**, 345 (2010).
9. T. J. Sherwin. *J of Phys Oc*, **18**, 1035 (1988).
10. M. E. Inall, T. P. Rippeth, T. J. Sherwin. *J of Geophys Res*, **105**, 8687 (2000).
11. P. G. Baines. *Deep-Sea Res. Part A - Oc Res Papers*, **29**, 307 (1982).
12. A. M. Althaus, E. Kunze, T. S. B. Sanford. *J of Phys Oc*, **33**, 1510 (2003).